



DOI: 10.32768/abc.20229150-65



Antiviral Drug 2-thio-6-azauridine Sensitizes Paclitaxel-Resistant Triple Negative Breast Cancer Cells by Targeting Mammosphere Formation and ABC Transporters

Rakshmitha Marni^a, Murali Mohan Gavara^a, Anindita Chakraborty^b, Rama Rao Malla^{*a}^aCancer Biology Lab, Dept of Biochemistry and Bioinformatics, Institute of Science, GITAM, Visakhapatnam, India^bRadiation Biology, UGC-DAE-CSR, Kolkata Centre, Kolkata, India

ARTICLE INFO

Received:

29 July 2021

Revised:

09 September 2021

Accepted:

11 October 2021

Keywords:ABC transporters,
CD151,
paclitaxel,
TNBC,
2-thio-6-azauridine

ABSTRACT

Background: 2-thio-6-azauridine (TAU) is a nucleoside analog and potential antiviral drug. The antiproliferative activity of TAU has been evaluated in limited cancer cell lines. The present study is aimed to evaluate the effect of TAU on drug sensitization mechanism in paclitaxel (PTX) resistant triple-negative breast cancer (TNBC) cells.

Methods: The cell death mechanism was determined using MTT, BrdU incorporation, apoptosis, and DNA damage Western blot and RT-PCR assays. A specific ELISA method was used to determine the caspase-3 activity and expression levels of MRP1, MDR1, BCRP, and MRP8. Western blot analysis was used to assess the expression of CD151, MRP1, MDR1, and BCRP in CD151 overexpressing PTX-resistant TNBC cells.

Results: The combination of TAU and PTX (10:20nM) synergistically inhibited the 50% viability of 12-fold PTX-resistant TNBC cells. Mechanistically, the combination inhibited the proliferation by arresting the cell cycle at the G2M phase and induced apoptosis by altering cell integrity and nuclear morphology as well as damaging DNA. The combination sensitized the PTX-resistant TNBC cells by increasing BAX and decreasing Bcl-2 expression, activating caspase-3, and reducing the expression of ABC transporters MRP1 and MDR1. The combination reduced the expression of MRP1 and MDR1 in CD151 overexpressing PTX-resistant TNBC cells, indicating the role of CD151 in TAU mediated sensitization of PTX-resistant TNBC cells. The combination also reduced the mammosphere formation efficiency of PTX-resistant TNBC cells.

Conclusion: Overall, the present study illustrated the promising ability of TAU in sensitizing drug-resistant TNBC cells to PTX.

Copyright © 2022. This is an open-access article distributed under the terms of the [Creative Commons Attribution-Non-Commercial 4.0](https://creativecommons.org/licenses/by-nc/4.0/) International License, which permits copy and redistribution of the material in any medium or format or adapt, remix, transform, and build upon the material for any purpose, except for commercial purposes.

INTRODUCTION

Triple-negative breast cancer (TNBC) is a clinically challenging heterogeneous subtype with poor differentiation, high proliferation ability, reduced five-year survival, increased relapse, and rapid drug

resistance development.¹ Among the subtypes, 10–20% is TNBC, which is highly aggressive due to the absence of typical hormone receptors and amplified Her2/neu. Paclitaxel (PTX) is a first-line chemotherapeutic drug for breast cancers. Approximately 1/3 of PTX-resistant breast cancers are triple-negative.

The combination of PTX with conventional chemotherapeutics was reported to enhance the survival of TNBC patients. The combination of PTX with a weekly dose of 5-Fluorouracil exhibited high efficacy against metastatic breast cancer in the phase II study.²

***Address for correspondence:**

Rama Rao Malla
Cancer Biology Lab, Dept of Biochemistry and Bioinformatics,
Institute of Science, GITAM, Visakhapatnam, India
Tel: +7386168249
Email: dr.rrmalla@gmail.com



Several clinical trials explored the possibility of combining the PTX with other cytotoxic drugs with proven efficacy against breast cancer.²⁻⁴ However, the development of resistance limited conventional therapeutics in combination with PTX against TNBC.⁵ Thus, elucidating the molecular mechanism of the PTX resistance and developing a new combination drug therapy for TNBC are urgently needed to decrease TNBC related mortality.

The integration of targeted and conventional antitumor chemotherapeutics could support the design of combination strategies for breast cancer treatment.⁶ Naturally-derived small molecules are being documented to discover cancer drugs.⁷ Previously, 2-thio-6-azauridine (TAU) was reported to be an antiviral agent against viruses.⁸ It is known to inhibit HIV-1 infection in HeLa cells and antitumor agents against L1210 Leukemia.^{9,10} TAU also targeted CD151 and inhibited the viability of the MDA-MB-231 cells.¹¹

Therefore, the development of novel combinations containing PTX with targeted therapeutics to combat drug-resistant TNBC is the focus of current research. This study is intended to establish the role of TAU in sensitizing PTX-resistant MDA-MB-231 (mesenchymal stem-like; basal B) and -MDA-MB-468 (basal-like 1; basal A) TNBC cells. In the present study, we demonstrate that a combination of TAU and PTX synergistically inhibits the viability of PTX-resistant TNBC cells. We show that, mechanistically, the combination inhibits the proliferation of PTX-resistant TNBC cells by arresting the cell cycle at the G2M phase and induced apoptosis by altering cell integrity, nuclear morphology, and damaging DNA. Another finding of the study is that the combination sensitizes the PTX-resistant TNBC cells by increasing BAX and decreasing Bcl-2 expression, activating caspase-3, and reducing the expression of ABC transporters MRP1 and MDR1. The combination also reduces the expression of MRP1 and MDR1/p-glycoprotein in CD151 overexpressing PTX-resistant TNBC cells indicating the role of CD151 in TAU mediated sensitization of PTX-resistant TNBC cells. The specific objective of this study is to sensitize PTX-resistant TNBC cells by targeting mammospheres formation and ABC transporters using antiviral drug TAU. Overall, the present study shows the effectiveness of TAU in the treatment of PTX-resistant TNBC cells.

METHODS

Cell lines and culture

TNBC cell lines (MDA-MB-231 and MDA-MB-468) were procured from NCCS (Pune, India) and cultured in DMEM (Invitrogen, USA) that contained 100 units of pen-strep antibiotic and 10% FBS (Invitrogen, USA) under 5% CO₂ atmosphere in the

incubator. Chemicals, TAU (98% pure) and PTX (97% pure), were commercially purchased (Sigma, USA).

Resistant cell line generation

An alternating, stepwise treatment method was used to develop PtxR-MDA-MB-231 and PtxR-MDA-MB-468 cell lines. The wild types of MDA-MB-231 and MDA-MB-468 cells were exposed to PTX at IC₃₀ for five days. Then, cells were grown in a medium without the drug for 5 days and again treated with PTX (IC₄₀). This step was repeated until the cells effectively expanded to 70% confluency under PTX (IC₄₀) treatment. Then, cells were maintained in the presence of PTX (IC₆₀) for 5 days. Single-cell clones (PtxR-/TNBC) were then attained by serial dilution in a 96-well plate and expanded.

Population doubling time (PDT)

PtxR/MDA-MB-231 and PtxR/MDA-MB-468 cells (2.0×10⁵ cells/ml) were cultured for 3 days, and the number of cells was determined by an automated cell counter (Invitrogen, USA) after staining with trypan blue at every 24 h. The PDT was calculated using an online algorithm software provided at <http://www.doubling-time.com>.

MTT cytotoxic assay

The PtxR/ TNBC cells (3.0×10³ cells/well) in a 96-well plate were treated with TAU (10-50nM) or PTX (10-50nM) or with various combinations (5:10, 10:20, 15:30 and 20:40nM) for 48h. 200ul of MTT solution (Sigma, USA) at a concentration of 5mg/ml was added to each well. After 3 h of incubation, absorbance has been measured by using a microplate reader at 570nm. Cytotoxicity was presented as a percent of untreated PtxR cells. Experiments were repeated three times (n=3), and the results were statistically expressed as mean ± SD.¹²

Drug interaction analysis

The synergistic, additive, or antagonistic cytotoxic impact of TAU and PTX was analyzed by the combination index (CI) method.¹³ The dose-effect curve for individual and combination treatments was generated and CI value for each treatment and consequent fraction affected (fa); the fraction results and data were calculated using CompuSyn software. The Fa–CI plots were constructed for evaluation of drug interactions by the simulation of CI values against fa levels ranging from 0.1 to 0.95. Experiments were repeated three times (n=3), and the results were statistically expressed as mean ± SD.

BrdU proliferation assay

The effect of TAU (10nM), PTX (20nM), and their effective combination (10:20nM) on PtxR/TNBC cell proliferation was assessed using the BrdU cell proliferation assay kit (Millipore, USA) as described earlier.¹⁴ Overnight-grown cells with 80% confluence were treated with TAU, PTX, and their combination



for 48h. Then, cells were treated with diluted BrdU for 12h. After fixing with a fixative solution, cells were incubated for 30min, followed by an anti-BrdU antibody (1:100) for 1h. Subsequently, cells were washed and incubated with conjugated secondary antibody (1:500) for 30min. Then, cells were incubated with tetramethylbenzidine in the dark for 15min. Immediately after adding a stop solution, the absorbance was determined using a multi-well plate reader at a dual-wavelength of 450 and 540nm. Experiments were repeated three times, and the results (n=3) were statistically expressed as mean \pm SD. Twenty PTX-resistant (PaxR/TNBC) cell line clones were recognized by limiting the dilution cloning method. The fold change of IC₅₀ compared to parental cell lines was plated using Origin software (Version, 2021).

Cell cycle analysis

Overnight-grown PtxR/TNBC cells with 80% confluence were exposed to a combination of TAU (10nM) and PTX (20nM) for 48h. After treatment, cells were washed with 1X phosphate buffer saline (PBS). Then, cells were exposed to propidium iodide containing RNase A (10 μ g/ml) for 30min in dark. The content of DNA in the cells (1.0x10⁴) at various phases was analyzed using a Flow Cytometer with \geq 10,000 events from each sample with Ex/Em wavelength of 488/530 nm. The distribution of cells in each phase was expressed in percent control.¹⁵ Experiments were repeated three times (n=3), and the results were statistically expressed as mean \pm SD.

Apoptosis by TUNEL assay

PtxR/TNBC cells were treated with TAU (10nM), PTX (20nM) and their combination (10:20nM) for 48 h. Then, cells were incubated with TUNEL reagent (R&D Systems, USA) for 1h. After staining with DAPI, cells were visualized under fluorescent microscopy. The percentage of green fluorescent cells (TUNEL-positive) was expressed by comparing with DAPI-stained cells.¹⁶ Experiments were repeated three times (n=3).

Dual AO/EtBr fluorescent staining

PtxR/TNBC cells (2.0x10³ cells /well) were treated with TAU (10nM), PTX (20nM) and their combination (10:20nM) for 48h. Untreated wells were considered as control. Cells were incubated with 100 μ g/ml of acridine orange (AO) and ethidium bromide (EtBr) for 1h. The morphological features of cells were recorded using a fluorescent microscope,¹⁷ and the percentage of cell damage index was calculated.¹⁸ Experiments were repeated three times (n=3).

Reverse transcriptase-PCR (RT-PCR) analysis

TRIzol reagent was used to isolate total RNA PtxR/TNBC cells.¹⁹ The isolated RNA was transformed to cDNA and amplified with PCR reagent (Invitrogen, USA) and gene-specific primers using RT-PCR set under conditions of initial denaturation

(95°C for 3min), 35 cycles of amplification: 94°C (45s); 55°C (30s); and 72°C (90s) and subsequent extension (72°C) for 10min. GAPDH was used as an internal control. The PCR products were resolved in 1% agarose electrophoresis gel.²⁰ The primers are GAPDH (F) 5'-GAGTCAACGGATTTGGTCGTAT-3' (R) 5'-AGCCTTCTCCATGGTGGTGAAGAC-3'; BAX (F) 5'-AGTGGCAGCTGACATGTTTT-3' (R) 5'-GGAGGAAGTCCAATGTCCAG-3'; Bcl-2 (F) 5'-CCGGGAGATCGTGATGAAGT-3' (R) 5'-ATCCCAGCCTCCGTTATCCT-3'. Experiments were repeated three times (n=3). The images were analyzed using Image J software and the results were statistically expressed as mean \pm SD.

Western blotting

After treatment, total protein was extracted with RIPA buffer (Sigma, USA) and resolved by SDS-PAGE, blot transferred to a Polyvinylidene fluoride (PVDF) membrane, and incubated with specific primary antibodies (1:1000) (Millipore, USA), followed by HRP tagged secondary antibodies (1:5000) (Millipore, USA).²¹ The densitometry was performed using Image J software (NIH, USA). Experiments were repeated three times (n=3).

Caspase 3 activity assay

Cleaved caspase-3 activity was assessed using colorimetry-based assay (Chemicon International Inc., Temecula, CA). Following the treatment, cell lysate from treated and untreated PtxR/TNBC cells was transferred to a microplate and incubated overnight with Ac-DEVD-pNA. Then, the activity of caspase 3 was determined.²² Experiments were repeated three times (n=3), and the results were statistically expressed as mean \pm SD.

ELISA for MRP-1, MDR1, BRCP, MRP-8

The MRP-1, MDR1, BRCP, and MRP-8 protein levels in PtxR/MDA-MB-231 and PtxR/MDA-MB-468 cells untreated or treated with a combination of TAU and PTX were measured using specific ELISA kits (MyBiosource.com, USA). Then, cells were washed with PBS and pelleted down by centrifugation (3000rpm, 5min). After lysis of cells, protein content was determined by the BCA method (Invitrogen, USA), and was distributed (20 μ g/well) into 96-well plate pre-coated with antibodies specific to MRP-1, MDR1/p-glycoprotein, BRCP, and MRP-8. Then, wells were incubated with HRP-conjugated secondary antibody for 30min. Following incubation, the reaction was arrested by the addition of stop solution, and absorbance was computed with an ELISA reader set at 450 nm. Experiments were repeated three times (n=3), and the results were statistically expressed as mean \pm SD.

Transfection with a CD151 expression plasmid

After attaining 80% confluence, PtxR/TNBC cells (approx. 3.0x10⁵ cells/well) in 6-well plates were transfected with 1 μ g of full-length CD151 expression



plasmid (OriGene, Cat# SC319271) using 3mL of Lipofectamine transfection reagent (Invitrogen, USA). After 24h of transfection, cells were washed and left untreated or treated with a combination of TAU and PTX for 48h. The expression of CD151, MRP1, MDR1, and BCRP proteins was determined by western blotting. Experiments were repeated three times (n=3).

Mammosphere assay

After treatment with a combination of TAU and PTX (10:20nM), PtxR/MDA-MB-231 and PtxR/MDA-MB-468 cells were supplemented with tumorsphere-XF medium and incubated in a humidified chamber at 37°C with 5% CO₂ for seven days. Then, TAU treated mammospheres were dissociated and cells were analyzed for the expression of CD44 and CD24 by flow cytometry. Untreated cells were served as control. After incubation, the image of tumorspheres were captured under phase-contrast microscopy at 40X magnification, and the number of mammospheres was counted. The mammosphere formation efficiency was calculated using the formula: Mammosphere formation efficiency (%) = No. of mammospheres per well / No. of cells seeded per well × 100. Experiments were repeated three times (n=3), and the results were statistically expressed as mean ± SD.

Statistical analysis

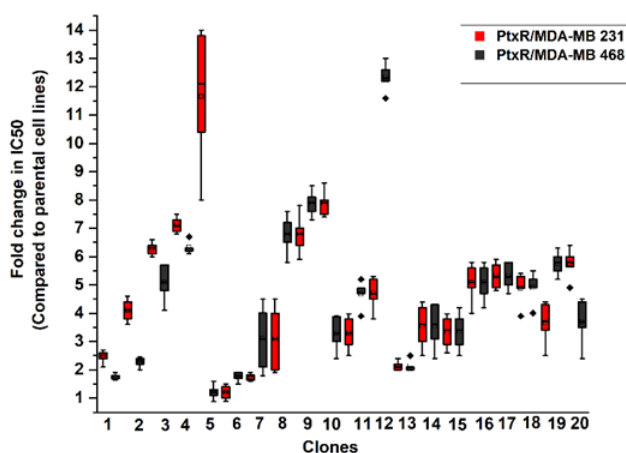
Every experiment was performed separately for three times, and the results were statistically expressed as mean ± SD. Statistically significant differences between control and target groups were determined using

the Student t-test. For statistical significance, confidence level was set at 5% (P<0.05).

RESULTS

Development of PTX-resistant cell clones

To develop PTX-resistant cell line clones, MDA-MB 231 and MDA-MB-468 cells were exposed to 19nM (IC₃₀), 24nM (IC₄₀), and 32nM (IC₆₀) of PTX in an intermittent and stepwise manner. Twenty PTX-resistant (PtxR/TNBC) cell line clones were recognized by limiting the dilution cloning method (Supplementary Figure 1). Only 12-fold PtxR/TNBC clones were chosen for further study. The cell-line growth curves were usually applied for the determination of population doubling time, maximum growth rate, and best time range for evaluating the effect of drugs.²³ As a preliminary study, population doubling time (PDT) of PtxR/MDA-MB-231 and PtxR/MDA-MB-468 cell clones and their parental cell types was evaluated by counting Trypan blue-stained cells.²⁴ The PDT of the PtxR/MDA-MB-231 cell clones was 72±1h, and that of MDA-MB-231 was 38±1h, whereas the PDT of PtxR/MDA-MB-468 cell clones was 72±1h and that of MDA-MB-468 cells was 47±1h (Supplementary Figure 2). High PDT indicates a slower growth rate of drug-resistant cells. The drug-resistant cells with reduced growth rate potentially alter the inhibitory activity of chemotherapeutic drugs compared to cells with a higher growth rate.²⁵



Supplementary Figure 1. Development of PTX-resistant cell lines. MDA-MB-231 cells were exposed first to 19nM (IC₃₀), followed by 24nM (IC₄₀) and finally 32nM (IC₆₀) in an intermittent manner for 5 days. Similarly, MDA-MB-468 cells were treated with 19.36 (IC₃₀), 26.1 (IC₄₀), followed by 38.74 (IC₆₀). Single clones were obtained by serial dilution, clones were grown to 80-90% confluency and IC₅₀ value of PTX was determined. Changes in IC₅₀ compared to parental cell lines were determined. The experiment was repeated 3 times (n=3). The results were expressed as mean ± SD.

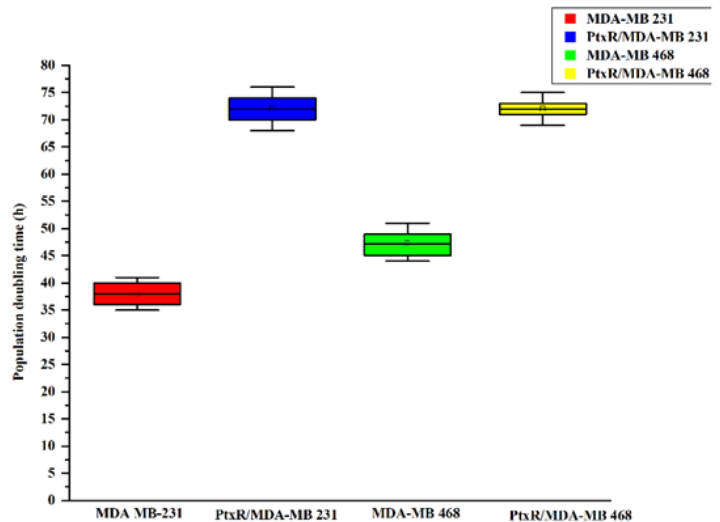
Effect of TAU and PTX on the viability of PtxR/TNBC cells

The nucleotide analog TAU reduced the proliferation of TNBC cells as well as CD151 expression.¹¹ The cell-line growth curves were usually applied for the determination of population doubling time, maximum growth rate, and best time range for evaluating the effect of drugs. The cells were treated with TAU (10-50nM) for 24h and IC₅₀ value was

precalculated as 29.91nM against MDA-MB-231 and 32.28nM against MDA-MB-468 cells. By considering the double-time, the cytotoxic effect of TAU or PTX on PtxR/MDA-MB231 and PtxR/MDA-MB-468 cells was determined at 65 h. The viability of untreated PtxR MDA-MB-231 and PtxR/MDA-MB-468 cells was considered 100%, and viability of treated cells was expressed in percent control.



Supplementary Figure 2. Population doubling time of PTX resistant TNBC cell clones. PtxR/MDA-MB-231 and PtxR/MDA-MB-468 cells (2×10^5 cells/ml) were cultured for 3 days, and the number of cells was determined by an automated cell counter (Invitrogen, USA) after staining with trypan blue at every 24h. The experiment was repeated 3 times ($n=3$). The PDT was calculated using an online algorithm software provided at <http://www.doubling-time.com>. The results were expressed as mean \pm SD.



The viability of PtxR/MDA-MB-231 and 468 cells was reduced with 10, 20, 30, 40 and 50nM of TAU, respectively at 72h (Figure 1a). The percentage of reduction in viability was shown in the Table 1. The result shows that the percentage of viability was decreased with an increase in the concentration of TAU from 10-50nM.

The viability of PtxR/MDA-MB-231 and 468 cells was also decreased with 10, 20, 30, 40 and 50nM of

PTX, respectively (Figure 1b). The percentage of reduction in viability was shown in the table 1. The result shows that the percentage of viability was decreased with an increase in the concentration of PTX from 10-50nM. The IC_{50} value of TAU was found to be 22.91 and 23.72nM against PtxR/MDA-MB-231 and PtxR/MDA-MB-468 cells, respectively, while PTX was 41 and 42nM, respectively at 72h.

Table 1. Effect of TAU and PTX on the viability of TNBC cells

Cell type	Concentration (nM)	Viability	
		TAU	PTX
PtxR/MDA-MB-231	10	37.86 \pm 0.44	27.30 \pm 0.32
	20	46.88 \pm 0.42	34.81 \pm 0.56
	30	59.96 \pm 0.62	48.72 \pm 0.21
	40	76.89 \pm 0.69	57.94 \pm 0.78
	50	85.84 \pm 0.72	61.92 \pm 0.51
PtxR/MDA-MB-468	10	33.46 \pm 0.28	26.12 \pm 0.64
	20	41.66 \pm 0.52	29.14 \pm 0.44
	30	56.64 \pm 0.54	43.32 \pm 0.86
	40	70.84 \pm 0.68	49.61 \pm 0.66
	50	79.84 \pm 0.64	54.42 \pm 0.97

The combination of TAU and PTX on the viability of PtxR/TNBC cells at 24h with 5:10, 10:20, 15:30, and 20:40nM was evaluated. The viability of PtxR/MDA-MB-231 cells was reduced by 35.24 \pm 0.82, 49.42 \pm 0.69, 75.22 \pm 0.39, 86.12 \pm 0.55 and 95.24 \pm 0.71%, whereas the viability for PtxR/MDA-MB-468 cells was reduced by 31.24 \pm 0.37, 47.31 \pm 0.29, 75.62 \pm 0.61 \pm 0.88, and 94.1 \pm 0.99% with 5:10, 10:20, 15:30 and 20:40nM combination of TAU and PTX, respectively (Figure 1c). The results indicated that the

viability of both PtxR/MDA-MB-231 and PtxR/MDA-MB-468 cells was reduced to 50% with a combination of TAU and PTX at 10:20nM combination. These results indicated that the combinational treatment of PTX and TAU was more significant at low doses than the individual drug treatments against PtxR/TNBC cells.

The synergistic cytotoxicity of TAU and PTX on PtxR/TNBC cells was calculated by the combination index method, and the combination index (CI) was



determined.¹⁵ The CI values from 0 to 3 and their corresponding effect levels were plotted in combination index curve (Fa–CI plot) (Figures 1d and e). The CI index at actual experimental points was 0.22, 0.94, 0.85 and 0.90 and Fa was 0.22, 0.96, 0.82 and 0.96 at 5:10, 10:20, 15:30 and 20:40nM for combination of TAU and PTX for PtxR/MDA-MB-231 cells. The CI index of TAU and PTX for PtxR/MDA-MB-468 cells was 0.32, 0.31, 0.57 and 0.79, whereas, Fa value was 0.23, 0.30, 0.55 and 0.78. The CI index was less than 1, indicating a synergistic interaction between TAU and PTX against PtxR/TNBC cells.¹³

Effect of TAU and PTX on proliferation of PtxR/TNBC cells

BrdU incorporation assay was used to assess the effect of TAU and PTX on the proliferation of PtxR/TNBC cells. The BrdU positive PtxR/MDA-MB-231 and PtxR/MDA-MB-468 cells were decreased by 62.44 ± 0.45 and $59.21 \pm 0.67\%$, respectively with

10nM of TAU and 41.52 ± 0.22 and $42.12 \pm 0.54\%$, respectively, with 20nM PTX and 96.42 ± 0.19 and $95.34 \pm 0.79\%$, respectively, with combination of TAU and PTX (10:20nM) (Figure 1f). The Trend analysis (Microsoft Excel, version 2016) of results indicate that TAU caused a significant ($P < 0.05$) decrease in the PtxR/TNBC cell proliferation with a combination of PTX compared to individual treatments ($P < 0.10$) (Supply Figure 3). The cell cycle drives the proliferation of cells. The halting of cell cycle progression inhibits tumor cell proliferation.²⁶ To determine the suppression of proliferation was caused by the cell cycle arrest, the effect of TAU and PTX on cell cycle progression of PtxR/TNBC cells was evaluated. The results show that the combination of TAU and PTX (10:20nM) arrested both PtxR/TNBC cell types at the G2M phase of the cell cycle (Figs. 2a and b).

Figure 1. Paclitaxel resistant MDA-MB-231 and MDA-MB-468 cells (5×10^3 /well) were treated with TAU (a) or PTX (b) at 10-50nM concentration for 48h and cytotoxicity was determined by MTT assay. Viability was expressed in percent control, mean \pm SD ($n=3$) and $*P < 0.05$. (c) Effect of combination of TAU and PTX on the viability of PtxR/MDA-MB-231 and PtxR/MDA-MB-468 cells at 5:10, 10:20, 15:30 and 20:40nM combination in 48h. The results were expressed as percent control from three independent experiments, as mean \pm SD ($n=3$) and statistical significance was set at $P < 0.05$. Combinational index values of TAU and PTX on PtxR/MDA-MB-231 (d) and PtxR/MDA-MB-468 (e) were calculated by the method of Chou–Talalay using CompuSyn software. (f) Effect of TAU, PTX and combination of TAU and PTX on the proliferation of PtxR/MDA-MB-231 and PtxR/MDA-MB-468 cell lines. Cells (5×10^3 /well) were treated with TAU (10nM), PTX (20nM) and combination of TAU and PTX (10:20nM) for 48h. Cell proliferation was determined by BrdU incorporation assay and results were represented as BrdU positive cells in % control. Results from three independent experiments were shown as mean \pm SD ($n=3$) and statistical significance was set at $P < 0.05$.

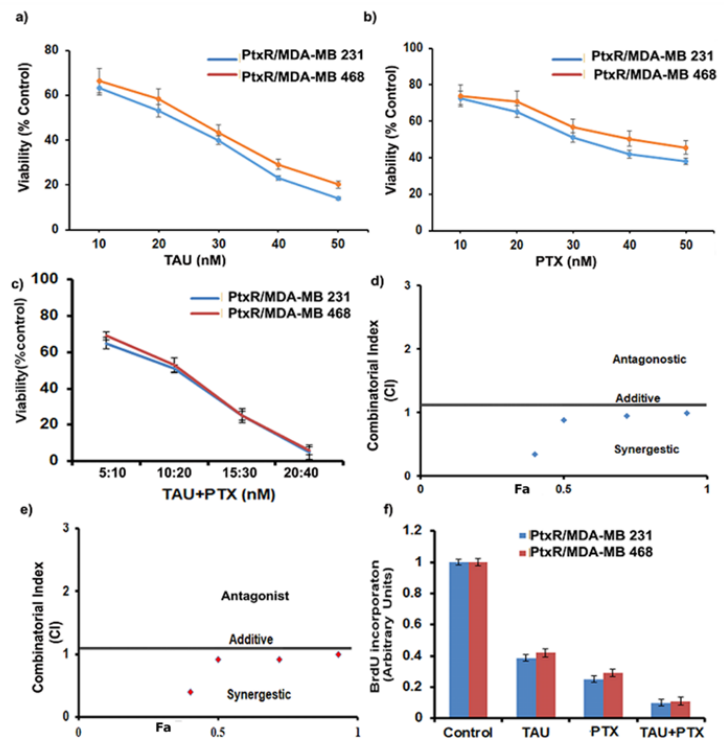


Figure 1

Effect of TAU and PTX on the integrity of PtxR/TNBC cell lines

To investigate whether the inhibition of cell proliferation was due to cell death, morphological changes in PtxR/TNBC cells were assessed after 48 h of treatment with TAU and PTX. The results showed that the combination treatment of TAU and PTX altered the morphology of both PtxR/MDA-MB-231 (Figure 2c) and PtxR/MDA-MB-468 cells (Figure 2d). The impact of TAU and PTX on the integrity of PtxR/TNBC cells was determined by the differential

staining method using AO/EtBr. AO stains both viable and non-viable cells, while EtBr stains only non-viable cells. Accordingly, the nuclei of untreated PtxR/TNBC cells were only stained with AO and exhibited green fluorescence. However, the nuclei of TAU and PTX treated cells exhibited orange fluorescence by staining with both AO and EtBr. This shows the loss of integrity of both PtxR/TNBC cells (Figures 2e and f) with a combination of TAU and PTX. The cell damage index was calculated from the score of non-viable and viable



PtxR/MDA-MB-231 and PtxR/MDA-MB-468 cells as 61.01 ± 0.08 and $59.45 \pm 0.89\%$, respectively.

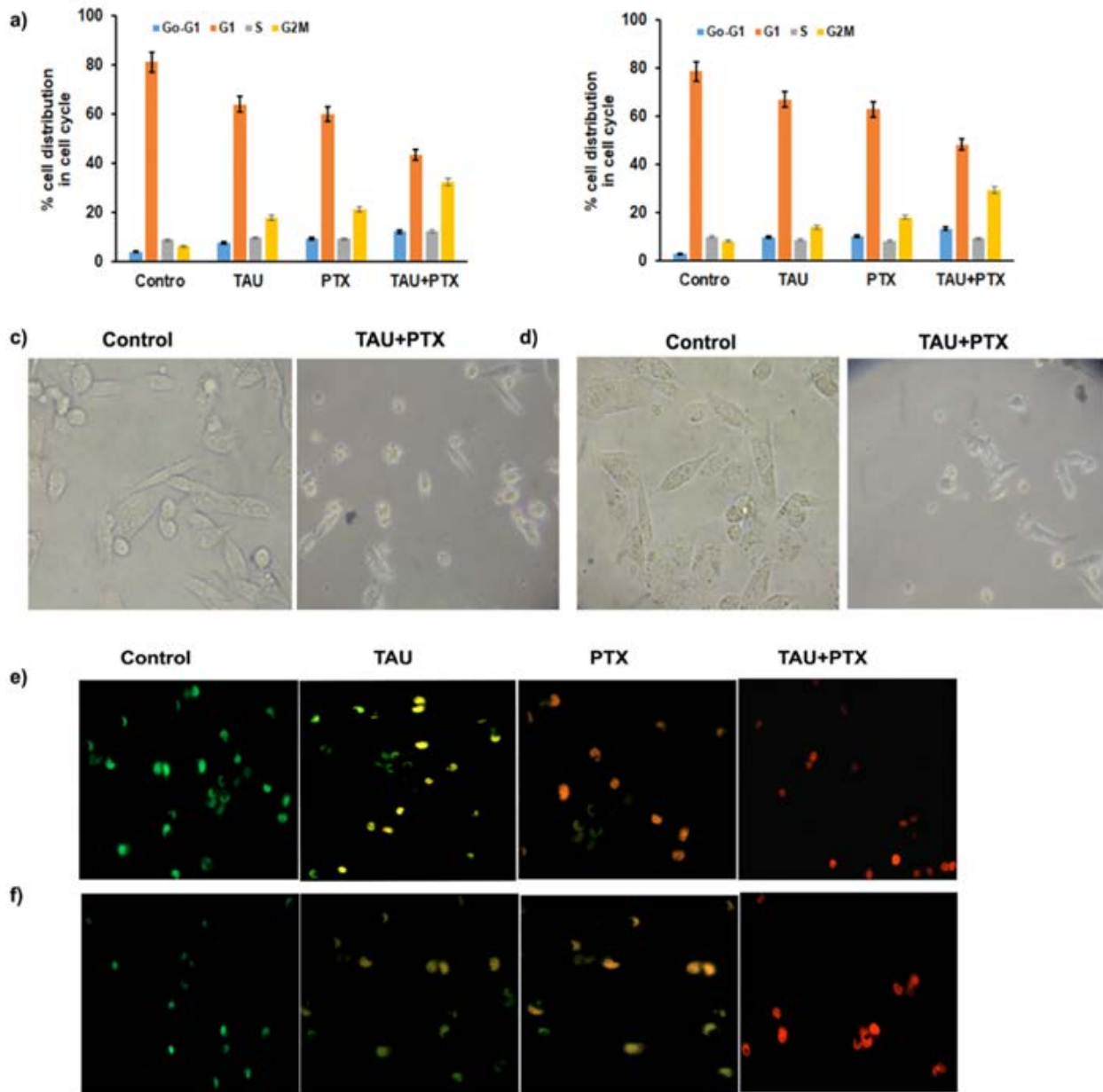
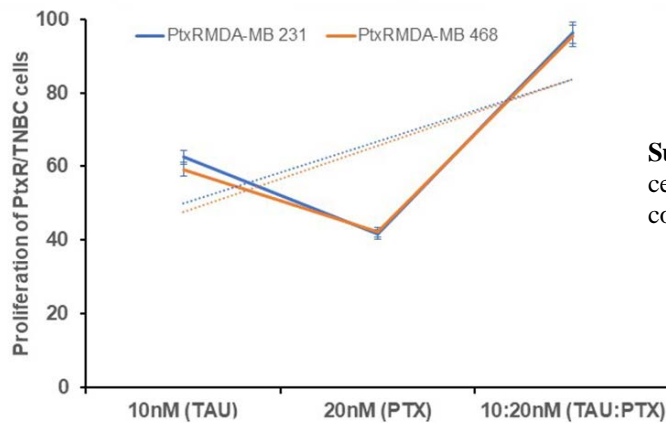


Figure 2

Figure 2. Effect of TAU and PTX on the integrity of PtxR/TNBC cells. Cell cycle distribution of PtxR/MDA-MB-231 (a) and PtxR/MDA-MB-468 cells (b). PtxR/MDA-MB-231 and PtxR/MDA-MB-468 cells were treated with TAU (10nM), PTX (20nM), and their combination (10:20nM) for 48h. Propidium iodide-stained cells (1.0×10^5) were analyzed for DNA content using flow cytometry. The data represent one of three independent experiments. Values are mean \pm SD of three different experiments. Effect of TAU and PTX on the morphology of PtxR/MDA-MB-231 (c) and PtxR/MDA-MB-468 (d). After 48h of treatment, cell morphology was captured under a phase-contrast microscope at 40X resolution. PtxR/MDA-MB-231 (e) and PtxR/MDA-MB-468 (f) cells were treated with TAU (10nM), PTX (20nM) and combination of TAU and PTX (10:20nM) for 48h. Cells were stained with AO and EtBr and images were captured under the fluorescent microscope at 20x magnification. Green fluorescence indicates live cells and orange-red fluorescence indicates dead cells. The data shown are from a representative experiment.



Supplementary Figure 3. Trend analysis of PtxR/TNBC cell proliferation with TAU (10nM), PTX (10nM) and combination of TAU and PTX (10:20nM).

Effects of TAU and PTX apoptosis in PtxR/TNBC cells

Apoptosis is an important mechanism that contributes to reduced tumor growth. TUNEL assay is used to evaluate TAU and PTX induced cell death. The 3' OH nicks of DNA labeled with TUNEL exhibited green fluorescence. The findings indicate that the PtxR/TNBC cells exhibited a significant number of TUNEL-positive cells with a combination of TAU and PTX (10:20nM) (Figures 3 a and b). The percentage of TUNEL positive untreated, TAU, PTX and TAU+PTX treated PtxR/MDA-MB-231 cells was 7.83 ± 0.73 , 54.62 ± 0.29 , $52.16 \pm 0.62\%$ and $72.22 \pm 0.83\%$, respectively. However, the percentage of untreated, TAU, PTX and TAU+PTX treated TUNEL positive PtxR/MDA-MB-468 cells was 9.14 ± 0.14 , 39.84 ± 0.47 , $39.14 \pm 0.29\%$ and $70.24 \pm 0.16\%$, respectively (Figure 3c).

To understand the TAU and PTX induced apoptotic mechanism, the expression of the apoptotic related genes, BAX and Bcl-2, was examined by RT-PCR (Figures 3d and e). The results show that the expression of BAX was moderately increased with separate treatments of TAU and PTX but significantly increased with the combination of TAU and PTX in both PtxR/MDA-MB-231 and PtxR/MDA-MB-468 cells. However, the expression of Bcl-2 was slightly decreased with TAU, but moderately with PTX and significantly with a combination of TAU and PTX. The comparative expression of BAX in PtxR/MDA-MB-231 was 1.27, 1.29, and 1.45-folds, respectively, and MDA-MB-468 cells were 1.42, 1.53, 1.93-folds with TAU, PTX, and combination of PTX and TAU, respectively, whereas controls were 0.35- and 0.81-folds, respectively. However, Bcl2 expression was 0.78-, 0.76- and 0.57-folds in PtxR/MDA-MB-231 cells and 0.76-, 0.75-, 0.62-folds in PtxR/MDA-MB-468 cells with TAU, PTX, and combination of PTX

and TAU, respectively, while untreated controls were 1.31- and 1.13-folds, respectively (Figure 3f).

The expression pattern of Bcl-2, as well as BAX proteins, was analyzed by immunoblotting (Figures 3g & h). The results showed that the expression of BAX protein was heightened in both PtxR/MDA-MB-231 and PtxR/MDA-MB-468 cells with TAU, PTX, and more significantly with a combination of TAU and PTX compared to untreated controls. However, the expression of Bcl-2 was decreased with all three treatments compared to untreated controls. The expression of BAX was enhanced by 1.41, 1.51- and 1.6- folds in PtxR/MDA-MB-231, whereas 1.50-, 1.57- and 1.69- folds in PtxR/MDA-MB-468 with TAU, PTX, and combination of TAU and PTX, respectively, compared to controls ($P^* < 0.05$). However, the expression of Bcl-2 protein was diminished by 1.3-, 1.21- and 0.9-folds in PtxR/MDA-MB-231 and 1.7-, 1.1- and 1.1-folds in PtxR/MDA-MB-468 cell with TAU, PTX, and combination of TAU and PTX, respectively, in comparison to the control (Figure 3i). The TAU and PTX induced apoptosis in PtxR/TNBC cells was confirmed by determining the active caspase3 levels using the ELISA method. The results showed that functional caspase levels were increased to 40 ± 2.34 , 61 ± 3.11 , and 80 ± 4.22 with TAU, PTX, and combination of TAU and PTX in PtxR/MDA-MB-231 cells, whereas the levels 42 ± 2.73 , 63 ± 3.28 , and 82 ± 4.36 with TAU, PTX and combination of TAU and PTX in PtxR/MDA-MB-468 cells (Figure 3j).

Effects of TAU and PTX drug resistance mechanism of PtxR/TNBC cells

ELISA was used to determine the effect of the combination of TAU and PTX on ABC transporters, MRP1, p-glycoprotein (MDR1), BCRP, and MRP8 levels, since these proteins have been reported to be involved in the development of drug resistance in breast cancer.^{27,28} The results display that the expression level of MRP1 was 0.11 and 0.12ng/mL of lysate



from TAU+PTX treated PtxR/MDA-MB-231 and PtxR/MDA-MB-468 cells, respectively, while untreated PtxR/MDA-MB-231 and PtxR/MDA-MB-468 cells showed 0.38 and 0.36ng/mL of cell lysate, respectively (Figure 4a). In addition, the levels of BCRP were 0.28 and 0.31ng/mL in lysate from untreated PtxR/MDA-MB-231 and PtxR/MDA-MB-468 cells, while 0.09 and 0.07ng/mL in TAU+PTX treated cells (Figure 4b). Further, the expression levels of MRP8 were 0.42 and 0.41ng/mL lysate from untreated PtxR/MDA-MB-231 and PtxR/MDA-MB-468 cells, respectively, whereas 0.13 and 0.11ng/mL lysate from TAU+PTX treated PtxR/MDA-MB-231 and PtxR/MDA-MB-468 cells (Figure 4c). The levels of MDR1 were 0.39 and 0.36ng/mL of lysate from untreated PtxR/MDA-MB-231 and PtxR/MDA-MB-

468 cells, respectively, whereas 0.04 and 0.06ng/mL of lysate from TAU+PTX treated PtxR/MDA-MB-231 and PtxR/MDA-MB-468 cells (Figure 4d).

As TAU targets CD151 in TNBC cells,¹¹ and drug-resistant proteins in PTX resistant TNBC cells, the possible role of CD151 in drug resistance was further explored. For this study, CD151 was overexpressed in PTX resistant TNBC cell types, and the expression of ABC transporters was determined by western blot analysis. The results showed that the expression of ABC transporters MRP1, MDR1, and BCRP levels were significantly reduced with a combination of TAU and PTX treatment in CD151 overexpressing PtxR/MDA-MB-231 and PtxR/MDA-MB-468 cells (Figures 4e and f).

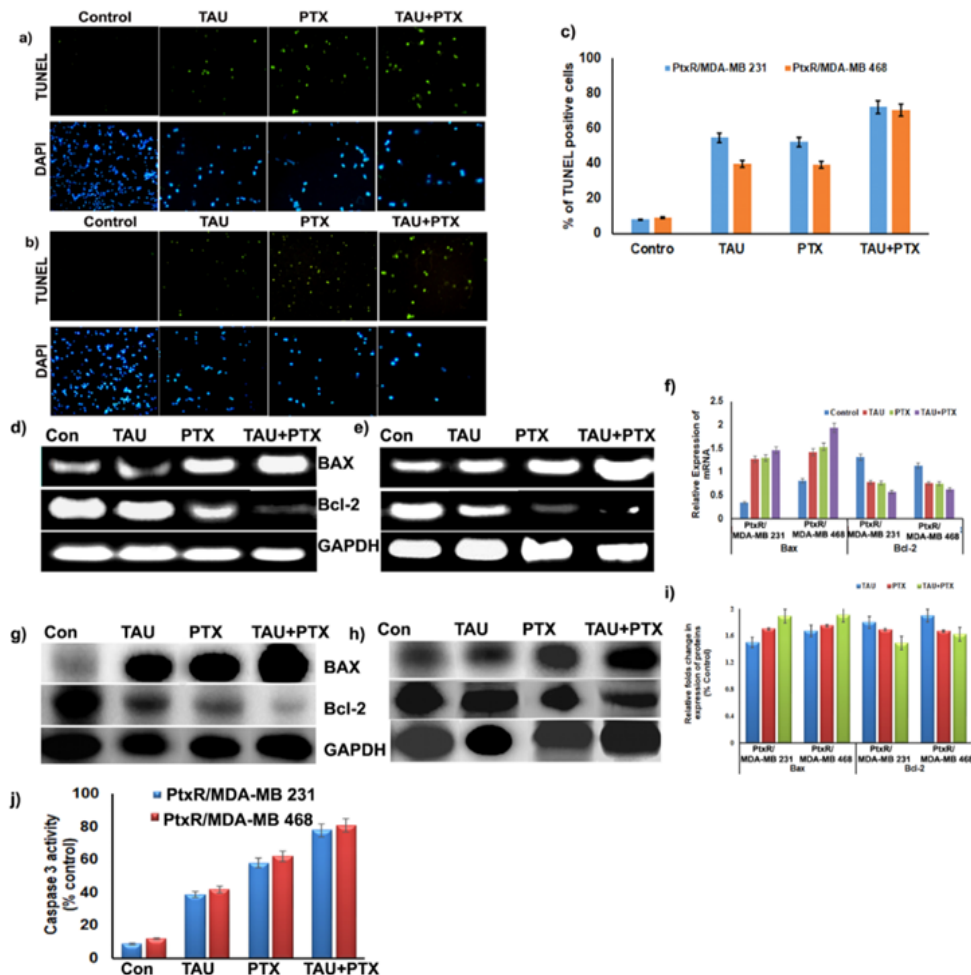


Figure 3

Figure 3. Effect of TAU and PTX on the induction of apoptosis in PtxR/TNBC cell lines. PtxR/MDA-MB-231 (a) and PtxR/MDA-MB-468 (b) were treated with TAU (10nM), PTX (20nM) and combination of TAU and PTX (10:20nM) for 48h. Cells were stained with TUNEL reagent. The data shown are from a representative experiment. c) Quantification of apoptotic cells expressed as the percentage of TUNEL positive cells compared to DAPI stained cells. mRNA expression of BAX and Bcl-2 compared with GAPDH on MDA-MB-231(d) and MDA-MB-468 cells (e). Quantification of BAX, and Bcl-2 mRNA levels by Reverse Transcriptase-PCR (f). The values were represented using Image J analysis. Relative Expression of BAX and Bcl-2 proteins in TAU and PTX treated MDA-MB-231 (g) and MDA-MB-468 cells (h) by performing western blotting. Relative folds changes in the expression of apoptotic proteins in comparison with GAPDH. The results were interpreted in terms of fold change



using image J analysis (i). Caspase-3 activity in MDA-MB231 and MDA-MB468 cell lines (j) were treated and measured by ELISA. Bars represent the mean \pm SD (n=3), $P \leq 0.05$.

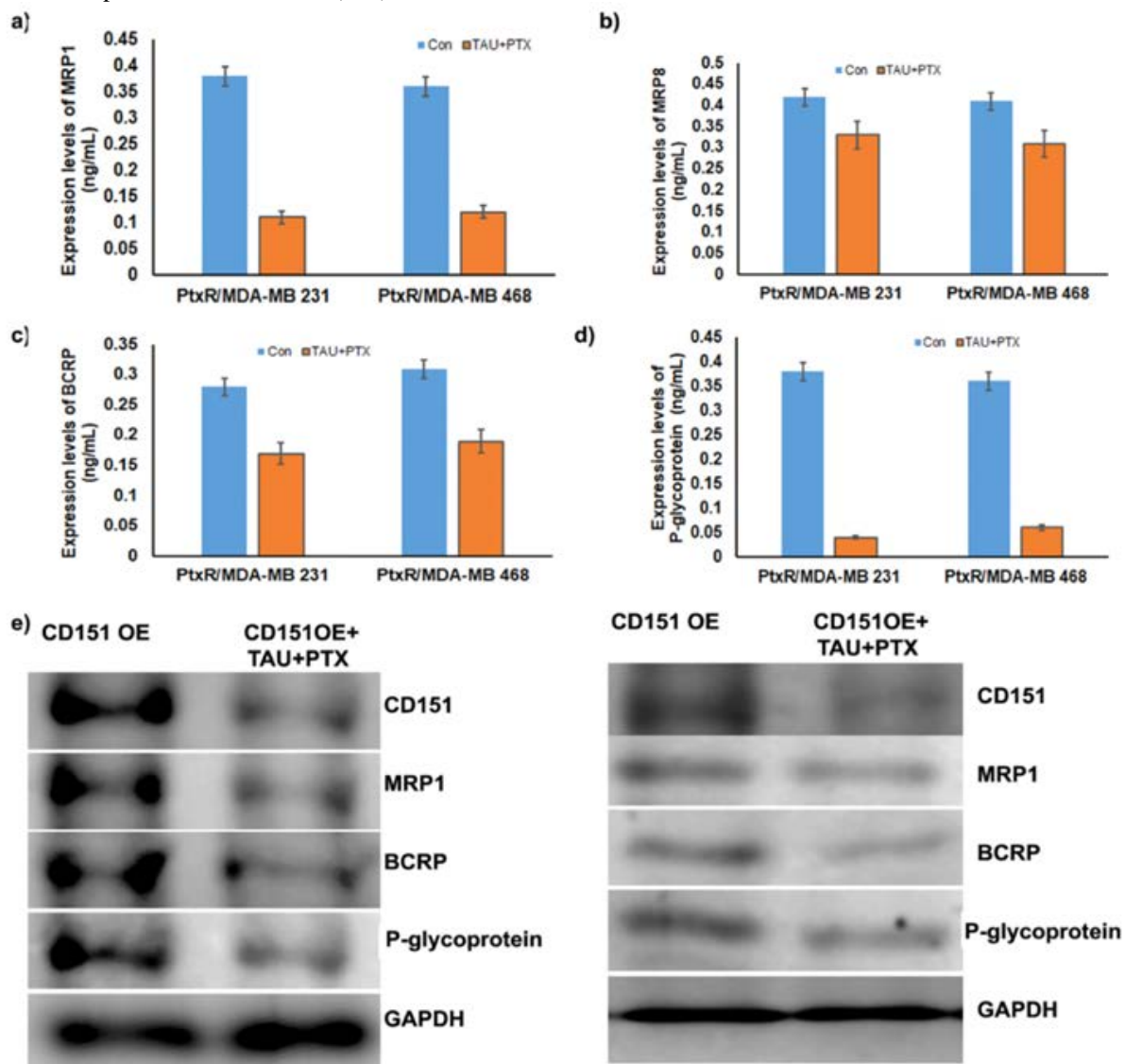


Figure 4. Effect of TAU and PTX on expression levels of ABC transport proteins. Effect of TAU and PTX on the expression of MRP 1 (a) BCRP (b) MRP-8 (c) and P-glycoprotein or MDR1 (d) The PtxR/MDA-MB-231 and PtxR/MDA-MB-468 cells were treated with a combination of TAU and PTX at 10:20nM. After 48 h treatment, the levels of MRP-1, MDR1, BCRP, and MRP-8 were determined by specific ELISA method. The cumulative data of each assay was from three independent experiments as shown as mean \pm SD (n=3), $P \leq 0.05$. Effect of TAU and PTX on the expression of MRP-1, BCRP and p-glycoprotein in CD151 overexpressed PtxR/MDA-MB-231 and PtxR/MDA-MB-468 cells (e) CD151 overexpressed cells were treated with a combination of TAU (10nM) and PTX (20nM) for 48h. The expression of MRP-1, BCRP and MDR1 were determined by western blotting. The cumulative data of each assay was from three independent experiments.

Studies have reported that breast tumors treated with chemotherapy are enriched with breast cancer stem cells (BCSCs), which are responsible for drug resistance and tumor relapse. If so, then targeting the BCSCs could be a promising strategy for reducing breast cancer growth. In view of this, stem cells were isolated from PtxR/MDA-MB-231 and PtxR/MDA-MB-468 cell clones and treated with the combination of PTX and TAU. The results showed that cells from the mammospheres expressed high levels of CD44 and low levels of CD24 [Data not shown]. One of the most characteristic features, mammosphere formation, was

assayed after 24h of treatment. The results showed that the size, as well as the number of the mammospheres, was significantly reduced in PtxR/MDA-MB-231 and PtxR/MDA-MB-468 cells with combination treatment compared to untreated controls (Figure 5a). The mammosphere formation efficiency was reduced to 36% in PtxR/MDA-MB-231 with the combination of TAU and PTX (10:20nM) compared to untreated control (100%), whereas 42% in PtxR/MDA-MB-468 compared to control (100%) (Figure 5b). These results indicated that a combination of TAU and PTX



sensitized stem cell character of drug-resistant TNBC cells.

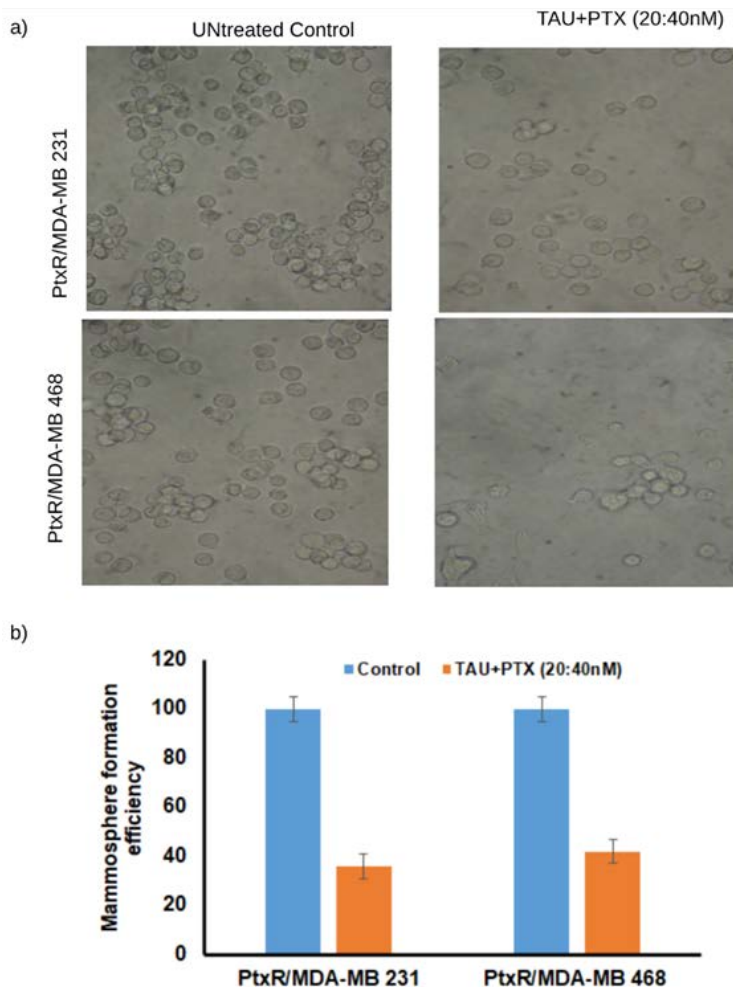


Figure 5. Effect of TAU and PTX on stemness of drug resistant TNBC cells. Effect of TAU and PTX on mammosphere formation (a) mammosphere formation efficiency (b). After treatment with combination of TAU and PTX (20:40nM), PtxR/MDA-MB-231 and PtxR/MDA-MB-468 cells were supplemented with tumorsphere-XF medium and incubated in a humidified chamber at 37°C with 5% CO₂ for seven days. Untreated cells were served as control. After incubation, the image of tumorspheres was captured under phase-contrast microscopy at 40X magnification and number of mammospheres was counted. The mammosphere formation efficiency was calculated using the formula: Mammosphere formation efficiency (%)=No. of mammospheres per well/No. of cells seeded per well×100.

DISCUSSION

Studies have reported that anthracyclines, alkylating agents, taxanes, and platinum agents show significant treatment benefits to TNBC patients.^{29,30} Studies have reported that chemotherapy using PTX improve the outcome of TNBC but brought limited clinical benefits due to the development of resistance.^{31,32} Studies have also reported that PTX induces apoptosis by binding in the Bcl-2 loop domain.³³ PTX with various combinations has been evaluated in patients with TNBC.³³⁻³⁹ Co-delivery of PTX and cisplatin using hydrogel showed synergistic effect on MDA-MB-231 cells by inducing apoptosis.⁴⁰

A recent clinical trial has reported on the use of PTX with the combination of targeted agents,⁴¹ which disrupt microtubules,⁴² induce DNA damage,⁴³ inhibit cell cycle,⁴⁴ induce apoptosis,⁴⁵ and reduce angiogenesis.⁴⁶ Earlier studies have demonstrated that anti-angiogenic agents, tyrosine kinase inhibitors, and EGFR inhibitors, along with chemotherapy, show moderate gains and have a similar effect on the survival of TNBC patients.⁴⁷

McDermott *et al.* (2014) have described that a 2- to 12-fold increase in drug resistance is clinically relevant acquired drug resistance.⁴⁸ Generally, clinically-related drug-resistant cell lines can be developed by growing continuously in the presence of the drug. In the present study, MDA-MB-231 and MDA-MB-468 cell lines with 12-fold resistance to PTX were developed by intermittent and alternative exposure to PTX. Hence, the developed PtxR/TNBC cell lines are clinically relevant models for drug discovery studies. The PTX resistant TNBC cells exhibited a higher population doubling time (PDT) compared to normal TNBC cells.

Generally, increased cell proliferation and reduced apoptosis are associated with drug resistance. Hence, we exploited these cellular functions to study the impact of TAU and PTX on PtxR/TNBC cells. For optimization of dose schedule, the experiments of screening for the optimal combination ratio of TAU and PTX were carried out by MTT and CI assays. This study observed significant cytotoxicity against PtxR/TNBC cell lines with a combination of TAU and



PTX compared to individual agents. Analysis of interaction between TAU and PTX using CompuSyn software revealed that a combination of TAU and PTX have significant cytotoxicity against PtxR/TNBC cell lines at 10:20nM concentration, which is 50% less than individual treatment concentrations. Further, the combination index (CI) ≤ 1 , indicated the synergetic effect of TAU and PTX on PtxR/TNBC cells in line with earlier studies.^{16,49}

Cell proliferation and cell cycle are critically related to the viability of cells.⁵⁰ Therefore, it is reasonably important to evaluate the effect of TAU and PTX on the proliferation and cell cycle of PtxR/TNBC cells. In the present study, we found that the combination of TAU and PTX induced morphological changes and loss of cell integrity, reducing the proliferation and inhibited cell cycle progression of PtxR/TNBC cells at the G2M phase. This inhibition may be mediated by loss of cell integrity, the hallmark of apoptosis.⁵¹

The Bcl-2 family proteins are key regulators of apoptosis, including Bcl-2 and BAX.⁵² Interestingly, Bcl-2 is found to be overexpressed while BAX is downregulated in TNBC cells.⁵³ It has also been reported that Bcl-2 promotes PTX resistance by enhancing the phosphorylation of Bcl2.⁵⁴ However, the upregulation of BAX sensitizes cancer cells to PTX by enhancing programmed cell death.⁵⁵ The combination of TAU and PTX enhanced the expression of BAX with simultaneous downregulation of Bcl2 in PtxR/TNBC cell lines. The ratio of Bcl-2 to Bax is the best-characterized regulator of apoptosis and contributes to caspase-3 mediated apoptosis.²¹ In line with this, the present study observed an increase in BAX to Bcl-2 ratio and activity of caspase-3 with a combination of TAU and PTX in PtxR/TNBC cell lines. The combination of TAU and PTX significantly reduced the expression of ABC transporters, MRP-1 and MDR1 but moderately BCRP in PtxR/TNBC. The expression of MRP1 and MDR1 was also decreased in CD151 overexpressed PtxR/TNBC cells, indicating that CD151 mediated PTX drug resistance.

CD151, a member of the tetraspanin family, plays a key role in the organization of signaling platform, tetraspanin enriched microdomains (TEM).⁵⁶ CD151 is associated with various partners in TEM and has a scaffolding role in cell survival, proliferation, adhesion, migration, and angiogenesis.⁵⁷ Targeted therapeutics against CD151 showed promising results in xenografts of solid tumors.⁵⁸ Blocking of LEL using specific monoclonal antibodies, recombinant EC2 domains, small molecule inhibitors, or silencing using siRNA inhibited the functions or disrupted the interaction of CD151 with its partners.^{59, 60} CD151 contributes to drug resistance in glioma initiating cells.⁶¹ Recently, Sooneyan *et al.*, (2019) have reported

that CD151 supports drug resistance in MDA-MB-231 TNBC cells.⁶²

From these studies, it is reasonable to conclude that the addition of two drugs of different mechanisms of action could dramatically augment cytotoxicity in TNBC cells. Further, the anticancer activity of TAU and PTX is probably complementary, which may contribute to a synergistic effect. Interestingly, PtxR/MDA-MB-231 and PtxR/MDA-MB-468 cell lines showed uniform response towards TAU and PTX, which may be due to the presence of common genes with a similar expression trend.⁶³ Breast tumors treated with PTX are enriched with cancer stem cells.⁶⁴ The present study observed that stem cells from PTX resistant TNBCs were sensitized by the combination treatment with PTX and TAU. An earlier study reported that PTX is ineffective in targeting BC stem cells, but a combination with other therapeutics sensitized the cells and reduced the number of mammospheres.⁶⁵ As far as we are aware, this is the first report to demonstrate the role of TAU in the sensitization of PTX resistance in TNBC cells.

CONCLUSION

In the current study, a traditionally and widely used anticancer drug, PTX, was selected as a model drug to develop resistance in MDA-MB-231, MDA-MB-468 cells. TAU, an inhibitor of CD151, showed significantly higher cytotoxicity in 12-fold PTX resistant TNBC cells with a 50% lower dose of PTX. This combination inhibited the most common drug-resistant cellular mechanisms, including cell proliferation, cell cycle progression of PtxR/TNBC cells, but induced apoptosis. Mechanistically, TAU and PTX combination reduced the expression of Bcl2, simultaneously inducing the BAX and caspase 3 expressions. They reduced the expression of common ABC transporters, MRP1 and MDR1, in PtxR and CD151 overexpressed TNBC cell lines. These findings show that TAU sensitizes 12-fold PTX resistant TNBC cells at lower effective dosages by inhibiting the expression of CD151. In conclusion, the present data describes the potential therapeutic value of CD151 in TAU-mediated sensitization of PTX-resistant TNBC cells.

ACKNOWLEDGEMENTS

The authors would like to thank UGC-DAE-CSR-KC/CRS/19/RB-04/1047, Kolkata for providing financial assistance, GITAM (Deemed to be University) for providing the facility for conducting this work. This research was supported by AMED under Grant Number JP21 ck0106555, and The Research Funding for Longevity Sciences (21-22) from the National Center for Geriatrics and Gerontology, Japan.

**CONFLICT OF INTEREST**

The authors declare no conflict of interest.

REFERENCES

1. Wahba HA, El-Hadaad HA. Current approaches in treatment of triple-negative breast cancer. *Cancer biology & medicine*. 2015;12(2):106-16. doi: 10.7497/j.issn.2095-3941.2015.0030.
2. Kucuk O, Pandya KJ, Skeel RT, Hochster H, Abeloff MD. Phase II study of cisplatin and 5-fluorouracil in previously treated metastatic breast cancer: an Eastern Cooperative Oncology Group study (PA 185). *Breast cancer research and treatment*. 1999;57(2):201-6. doi: 10.1023/a:1006229701954.
3. Zajdel A, Nycz J, Wilczok A. Lapatinib enhances paclitaxel toxicity in MCF-7, T47D, and MDA-MB-321 breast cancer cells. *Toxicology in vitro : an international journal published in association with BIBRA*. 2021;75:105200. doi: 10.1016/j.tiv.2021.105200.
4. Zhong P, Chen X, Guo R, Chen X, Chen Z, Wei C, et al. Folic Acid-Modified Nanoerythrocyte for Codelivery of Paclitaxel and Tariquidar to Overcome Breast Cancer Multidrug Resistance. *Molecular pharmaceutics*. 2020;17(4):1114-26. doi: 10.1021/acs.molpharmaceut.9b01148.
5. Thakur V, Kutty RV. Recent advances in nanotheranostics for triple negative breast cancer treatment. *Journal of Experimental & Clinical Cancer Research*. 2019;38(1):430. doi: 10.1186/s13046-019-1443-1.
6. Michelle Xu M, Pu Y, Weichselbaum RR, Fu YX. Integrating conventional and antibody-based targeted anticancer treatment into immunotherapy. *Oncogene*. 2017;36(5):585-92. doi: 10.1038/onc.2016.231.
7. Di L, Liu LJ, Yan YM, Fu R, Li Y, Xu Y, et al. Discovery of a natural small-molecule compound that suppresses tumor EMT, stemness and metastasis by inhibiting TGFbeta/BMP signaling in triple-negative breast cancer. *Journal of experimental & clinical cancer research : CR*. 2019;38(1):134. doi: 10.1186/s13046-019-1130-2.
8. Morrey JD, Smee DF, Sidwell RW, Tseng C. Identification of active antiviral compounds against a New York isolate of West Nile virus. *Antiviral research*. 2002;55(1):107-16. doi: 10.1016/s0166-3542(02)00013-x.
9. Li LH, Neil GL, Moxley TE, Olin EJ. Antitumor activity and mode of action of 2-thio-6-azauridine (NSC-146268) on L1210 leukemia. *Cancer chemotherapy reports*. 1974;58(3):345-52. doi: Not Available.
10. Loret EP, Darque A, Jouve E, Loret EA, Nicolino-Brunet C, Morange S, et al. Erratum to: Intradermal injection of a Tat Oyi-based therapeutic HIV vaccine reduces of 1.5 log copies/mL the HIV RNA rebound median and no HIV DNA rebound following cART interruption in a phase I/II randomized controlled clinical trial. *Retrovirology*. 2016;13(1):35. doi: 10.1186/s12977-016-0264-y.
11. Gavara MM, Zaveri K, Badana AK, Gugalavath S, Amajala KC, Patnala K, et al. A novel small molecule inhibitor of CD151 inhibits proliferation of metastatic triple negative breast cancer cell lines. *Process biochemistry*. 2018;66:254-62. doi: 10.1016/j.procbio.2017.12.004.
12. Kgg D, Kumari S, G S, Malla RR. Marine natural compound cyclo(L-leucyl-L-prolyl) peptide inhibits migration of triple negative breast cancer cells by disrupting interaction of CD151 and EGFR signaling. *Chemico-biological interactions*. 2019;315:108872. doi: 10.1016/j.cbi.2019.108872.
13. Fouquier J, Guedj M. Analysis of drug combinations: current methodological landscape. *Pharmacology research & perspectives*. 2015;3(3):e00149. doi: 10.1002/prp2.149.
14. Badana AK, Chintala M, Gavara MM, Naik S, Kumari S, Kappala VR, et al. Lipid rafts disruption induces apoptosis by attenuating expression of LRP6 and survivin in triple negative breast cancer. *Biomed Pharmacother*. 2018;97:359-68. doi: 10.1016/j.biopha.2017.10.045.
15. Badana A, Chintala M, Varikuti G, Pudi N, Kumari S, Kappala VR, et al. Lipid Raft Integrity Is Required for Survival of Triple Negative Breast Cancer Cells. *Journal of breast cancer*. 2016;19(4):372-84. doi: 10.4048/jbc.2016.19.4.372.
16. Kumari S, Mohan MG, Shailender G, Badana AK, Malla RR. Synergistic enhancement of apoptosis by coralyne and paclitaxel in combination on MDA-MB-231 a triple-negative breast cancer cell line. *Journal of cellular biochemistry*. 2019;120(10):18104-16. doi: 10.1002/jcb.29114.
17. Liu K, Liu PC, Liu R, Wu X. Dual AO/EB staining to detect apoptosis in osteosarcoma cells compared with flow cytometry. *Medical science monitor basic research*. 2015;21:15-20. doi: 10.12659/msmbr.893327.
18. Garrity MM, Burgart LJ, Riehle DL, Hill EM, Sebo TJ, Witzig T. Identifying and quantifying apoptosis: navigating technical pitfalls. *Modern pathology : an official journal of the United States and Canadian Academy of Pathology, Inc*. 2003;16(4):389-94. doi: 10.1097/01.mp.0000062657.30170.92.
19. Kumar AD, Bevara GB, Kaja LK, Badana AK, Malla RR. Protective effect of 3-O-methyl quercetin and kaempferol from *Semecarpus anacardium* against H2O2 induced cytotoxicity in lung and liver cells. *BMC complementary and alternative medicine*. 2016;16(1):376. doi: 10.1186/s12906-016-1354-z.



20. Malla RR, Gopinath S, Alapati K, Gorantla B, Gondi CS, Rao JS. uPAR and cathepsin B inhibition enhanced radiation-induced apoptosis in gliomaintiating cells. *Neuro-oncology*. 2012;14(6):745-60. doi: doi.org/10.1093/neuonc/nos088.
21. Malla R, Gopinath S, Alapati K, Gondi CS, Gujrati M, Dinh DH, et al. Downregulation of uPAR and cathepsin B induces apoptosis via regulation of Bcl-2 and Bax and inhibition of the PI3K/Akt pathway in gliomas. *PloS one*. 2010;5(10):e13731. doi: 10.1371/journal.pone.0013731.
22. Bevara GB, Naveen Kumar AD, Koteswaramma KL, Badana A, Kumari S, Malla RR. C-glycosyl flavone from *Urginea indica* inhibits proliferation & angiogenesis & induces apoptosis via cyclin-dependent kinase 6 in human breast, hepatic & colon cancer cell lines. *The Indian journal of medical research*. 2018;147(2):158-68. doi: 10.4103/ijmr.IJMR_51_16.
23. Assanga I, Lujan L. Cell growth curves for different cell lines and their relationship with biological activities. *International Journal of Biotechnology and Molecular Biology Research*. 2013;4(4):60-70. doi: Not Available
24. Shebaby W, Abdalla EK, Saad F, Faour WH. Data on isolating mesenchymal stromal cells from human adipose tissue using a collagenase-free method. *Data in brief*. 2016;6:974-9. doi: 10.1016/j.dib.2016.02.002.
25. Lovitt CJ, Shelper TB, Avery VM. Doxorubicin resistance in breast cancer cells is mediated by extracellular matrix proteins. *BMC Cancer*. 2018;18(1):41. doi: 10.1186/s12885-017-3953-6.
26. Mills CC, Kolb EA, Sampson VB. Recent Advances of Cell-Cycle Inhibitor Therapies for Pediatric Cancer. *Cancer research*. 2017;77(23):6489-98. doi: 10.1158/0008-5472.can-17-2066.
27. Alfarouk KO, Stock CM, Taylor S, Walsh M, Muddathir AK, Verduzco D, et al. Resistance to cancer chemotherapy: failure in drug response from ADME to P-gp. *Cancer cell international*. 2015;15:71. doi: 10.1186/s12935-015-0221-1.
28. Yamada A, Ishikawa T, Ota I, Kimura M, Shimizu D, Tanabe M, et al. High expression of ATP-binding cassette transporter ABCC11 in breast tumors is associated with aggressive subtypes and low disease-free survival. *Breast cancer research and treatment*. 2013;137(3):773-82. doi: 10.1007/s10549-012-2398-5.
29. Bilici A, Arslan C, Altundag K. Promising therapeutic options in triple-negative breast cancer. *Journal of BUON: official journal of the Balkan Union of Oncology*. 2012;17(2):209-22. doi: Not Available.
30. Isakoff SJ. Triple-negative breast cancer: role of specific chemotherapy agents. *Cancer journal (Sudbury, Mass)*. 2010;16(1):53-61. doi: 10.1097/PPO.0b013e3181d24ff7.
31. Lai H, Wang R, Li S, Shi Q, Cai Z, Li Y, et al. LIN9 confers paclitaxel resistance in triple negative breast cancer cells by upregulating CCSAP. *Science China Life sciences*. 2019. doi: 10.1007/s11427-019-9581-8.
32. Sprouse AA, Herbert BS. Resveratrol augments paclitaxel treatment in MDA-MB-231 and paclitaxel-resistant MDA-MB-231 breast cancer cells. *Anticancer research*. 2014;34(10):5363-74. doi: Not Available.
33. Ferlini C, Cicchillitti L, Raspaglio G, Bartollino S, Cimitan S, Bertucci C, et al. Paclitaxel directly binds to Bcl-2 and functionally mimics activity of Nur77. *Cancer research*. 2009;69(17):6906-14. doi: 10.1158/0008-5472.can-09-0540.
34. Torrisi R, Balduzzi A, Ghisini R, Rocca A, Bottiglieri L, Giovanardi F, et al. Tailored preoperative treatment of locally advanced triple negative (hormone receptor negative and HER2 negative) breast cancer with epirubicin, cisplatin, and infusional fluorouracil followed by weekly paclitaxel. *Cancer chemotherapy and pharmacology*. 2008;62(4):667-72. doi: 10.1007/s00280-007-0652-z.
35. Kaye S, Brown R, Gabra H, Gore M. *Emerging therapeutic targets in ovarian cancer*: Springer; 2011.
36. Burande AS, Viswanadh MK, Jha A, Mehata AK, Shaik A, Agrawal N, et al. EGFR Targeted Paclitaxel and Piperine Co-loaded Liposomes for the Treatment of Triple Negative Breast Cancer. *AAPS PharmSciTech*. 2020;21(5):151. doi: 10.1208/s12249-020-01671-7.
37. Schmid P, Rugo HS, Adams S, Schneeweiss A, Barrios CH, Iwata H, et al. Atezolizumab plus nab-paclitaxel as first-line treatment for unresectable, locally advanced or metastatic triple-negative breast cancer (IMpassion130): updated efficacy results from a randomised, double-blind, placebo-controlled, phase 3 trial. *The Lancet Oncology*. 2020;21(1):44-59. doi: 10.1016/s1470-2045(19)30689-8.
38. Kang C, Syed YY. Atezolizumab (in Combination with Nab-Paclitaxel): A Review in Advanced Triple-Negative Breast Cancer. *Drugs*. 2020;80(6):601-7. doi: 10.1007/s40265-020-01295-y.
39. Hsu MY, Hsieh CH, Huang YT, Chu SY, Chen CM, Lee WJ, et al. Enhanced Paclitaxel Efficacy to Suppress Triple-Negative Breast Cancer Progression Using Metronomic Chemotherapy with a Controlled Release System of Electrospun Poly-d-l-Lactide-Co-Glycolide (PLGA) Nanofibers. *Cancers*. 2021;13(13). doi: 10.3390/cancers13133350.



40. Davoodi P, Ng WC, Srinivasan MP, Wang CH. Codelivery of anti-cancer agents via double-walled polymeric microparticles/injectable hydrogel: A promising approach for treatment of triple negative breast cancer. *Biotechnology and bioengineering*. 2017;114(12):2931-46. doi: 10.1002/bit.26406.
41. Reguera-Nuñez E, Xu P, Chow A, Man S, Hilberg F, Kerbel RS. Therapeutic impact of Nintedanib with paclitaxel and/or a PD-L1 antibody in preclinical models of orthotopic primary or metastatic triple negative breast cancer. *Journal of Experimental & Clinical Cancer Research*. 2019;38(1):16. doi: 10.1186/s13046-018-0999-5.
42. Lee H, Jeon J, Ryu YS, Jeong JE, Shin S, Zhang T, et al. Disruption of microtubules sensitizes the DNA damage-induced apoptosis through inhibiting nuclear factor kappaB (NF-kappaB) DNA-binding activity. *Journal of Korean medical science*. 2010;25(11):1574-81. doi: 10.3346/jkms.2010.25.11.1574.
43. Woods D, Turchi JJ. Chemotherapy induced DNA damage response: convergence of drugs and pathways. *Cancer biology & therapy*. 2013;14(5):379-89. doi: 10.4161/cbt.23761.
44. Dickson MA, Schwartz GK. Development of cell-cycle inhibitors for cancer therapy. *Current oncology (Toronto, Ont)*. 2009;16(2):36-43. doi: 10.3747/co.v16i2.428.
45. Maire V, Nemati F, Richardson M, Vincent-Salomon A, Tesson B, Rigail G, et al. Polo-like kinase 1: a potential therapeutic option in combination with conventional chemotherapy for the management of patients with triple-negative breast cancer. *Cancer research*. 2013;73(2):813-23. doi: 10.1158/0008-5472.can-12-2633.
46. Luengo-Gil G, Gonzalez-Billalabeitia E, Chaves-Benito A, Garcia Martinez E, Garcia Garre E, Vicente V, et al. Effects of conventional neoadjuvant chemotherapy for breast cancer on tumor angiogenesis. *Breast cancer research and treatment*. 2015;151(3):577-87. doi: 10.1007/s10549-015-3421-4.
47. Yadav BS, Sharma SC, Chanana P, Jhamb S. Systemic treatment strategies for triple-negative breast cancer. *World journal of clinical oncology*. 2014;5(2):125-33. doi: 10.5306/wjco.v5.i2.125.
48. McDermott M, Eustace AJ, Busschots S, Breen L, Crown J, Clynes M, et al. In vitro Development of Chemotherapy and Targeted Therapy Drug-Resistant Cancer Cell Lines: A Practical Guide with Case Studies. *Frontiers in oncology*. 2014;4:40. doi: 10.3389/fonc.2014.00040.
49. Kumari S, Badana AK, Mohan GM, Shailender Naik G, Malla R. Synergistic effects of coralyne and paclitaxel on cell migration and proliferation of breast cancer cells lines. *Biomed Pharmacother*. 2017;91:436-45. doi: 10.1016/j.biopha.2017.04.027.
50. Gopinath S, Malla RR, Gondi CS, Alapati K, Fassett D, Klopfenstein JD, et al. Co-depletion of cathepsin B and uPAR induces G0/G1 arrest in glioma via FOXO3a mediated p27 upregulation. *PloS one*. 2010;5(7):e11668. doi: 10.1371/journal.pone.0011668.
51. Zhang Y, Chen X, Gueydan C, Han J. Plasma membrane changes during programmed cell deaths. *Cell research*. 2018;28(1):9-21. doi: 10.1038/cr.2017.133.
52. Malla RR, Gopinath S, Gondi CS, Alapati K, Dinh DH, Tsung AJ, et al. uPAR and cathepsin B downregulation induces apoptosis by targeting calcineurin A to BAD via Bcl-2 in glioma. *Journal of neuro-oncology*. 2012;107(1):69-80. doi: 10.1007/s11060-011-0727-x.
53. Williams MM, Cook RS. Bcl-2 family proteins in breast development and cancer: could Mcl-1 targeting overcome therapeutic resistance? *Oncotarget*. 2015;6(6):3519-30. doi: 10.18632/oncotarget.2792.
54. Ruvolo PP, Deng X, May WS. Phosphorylation of Bcl2 and regulation of apoptosis. *Leukemia*. 2001;15(4):515-22. doi: 10.1038/sj.leu.2402090.
55. Erdogan S, Doganlar O, Doganlar ZB, Turkecul K. Naringin sensitizes human prostate cancer cells to paclitaxel therapy. *Prostate international*. 2018;6(4):126-35. doi: 10.1016/j.pnrl.2017.11.001.
56. Serru V, Le Naour F, Billard M, Azorsa DO, Lanza F, Boucheix C, et al. Selective tetraspan-integrin complexes (CD81/alpha4beta1, CD151/alpha3beta1, CD151/alpha6beta1) under conditions disrupting tetraspan interactions. *The Biochemical journal*. 1999;340 (Pt 1):103-11. doi: Not Available.
57. Yang X, Li S, Zhong J, Zhang W, Hua X, Li B, et al. CD151 mediates netrin-1-induced angiogenesis through the Src-FAK-Paxillin pathway. *Journal of cellular and molecular medicine*. 2017;21(1):72-80. doi: 10.1111/jcmm.12939.
58. Ke AW, Zhang PF, Shen YH, Gao PT, Dong ZR, Zhang C, et al. Generation and characterization of a tetraspanin CD151/integrin alpha6beta1-binding domain competitively binding monoclonal antibody for inhibition of tumor progression in HCC. *Oncotarget*. 2016;7(5):6314-22. doi: 10.18632/oncotarget.6833.
59. Hemler ME. Targeting of tetraspanin proteins--potential benefits and strategies. *Nature reviews Drug discovery*. 2008;7(9):747-58. doi: 10.1038/nrd2659.
60. Bonnet M, Maisoniau-Besset A, Zhu Y, Witkowski T, Roche G, Boucheix C. Targeting the Tetraspanins with Monoclonal Antibodies in Oncology: Focus on Tspan8/Co-029. 2019;11(2). doi: 10.3390/cancers11020179.
61. Tilghman J, Schiapparelli P, Lal B, Ying M, Quinones-Hinojosa A, Xia S, et al. Regulation of



- Glioblastoma Tumor-Propagating Cells by the Integrin Partner Tetraspanin CD151. *Neoplasia* (New York, NY). 2016;18(3):185-98. doi: 10.1016/j.neo.2016.02.003.
62. Hwang S, Takimoto T, Hemler ME. Integrin-independent support of cancer drug resistance by tetraspanin CD151. 2019;76(8):1595-604. doi: 10.1007/s00018-019-03014-7.
63. Mudvari P, Ohshiro K, Nair V, Horvath A, Kumar R. Genomic insights into triple-negative and HER2-positive breast cancers using isogenic model systems. *PloS one*. 2013;8(9):e74993. doi: 10.1371/journal.pone.0074993.
64. Zhang S, Zhang H, Ghia EM, Huang J, Wu L, Zhang J, et al. Inhibition of chemotherapy resistant breast cancer stem cells by a ROR1 specific antibody. *Proc Natl Acad Sci U S A*. 2019;116(4):1370-7. doi: 10.1073/pnas.1816262116.
65. Das S, Mukherjee P, Chatterjee R, Jamal Z, Chatterji U. Enhancing Chemosensitivity of Breast Cancer Stem Cells by Downregulating SOX2 and ABCG2 Using Wedelolactone-encapsulated Nanoparticles. *Mol Cancer Ther*. 2019;18(3):680-92. doi: 10.1158/1535-7163.Mct-18-0409.

How to Cite This Article

Marni R, Gavara MM, Chakraborty A, Malla RR. Antiviral Drug 2-thio-6-azauridine Sensitizes Paclitaxel-Resistant Triple Negative Breast Cancer Cells by Targeting Mammosphere Formation and ABC Transporters. *Arch Breast Cancer*. 2022; 9(1):50-65.

Available from: <https://www.archbreastcancer.com/index.php/abc/article/view/446>